

# Polyethylene reinforced with keratin fibers obtained from chicken feathers<sup>☆</sup>

Justin R. Barone<sup>\*</sup>, Walter F. Schmidt

*USDA/ARS/ANRI/EQL, Bldg. 012, Rm. 1-3, BARC-West, 10300 Baltimore Ave. Beltsville, MD 20705, USA*

Received 15 January 2004; received in revised form 22 June 2004; accepted 22 June 2004

Available online 24 August 2004

## Abstract

Polyethylene-based composites were prepared using keratin fibers obtained from chicken feathers. Fibers of similar diameter but varying aspect ratio were mixed into low-density polyethylene (LDPE) using a Brabender mixing head. From uniaxial tensile testing, an elastic modulus and yield stress increase of the composite over the virgin polymer was observed over a wide range of fiber loading. Scanning electron microscopy revealed some interaction between the polymer and keratin feather fiber. In addition, the keratin fiber had a density lower than the LDPE used in this study resulting in composite materials of reduced density. The results obtained from mechanical testing are compared to theoretical predictions based on a simple composite material micromechanical model. Published by Elsevier Ltd.

*Keywords:* A. Fibers; A. Polymer-matrix composites; A. Short-fiber composites; B. Mechanical properties; B. Microstructure

## 1. Introduction

There has been recent interest in developing composites based on short-fibers obtained from agricultural resources. These fibers are usually of lower density than inorganic fibers, environmentally-friendly, and relatively easy to obtain. It is anticipated that the fibers would not contribute to the wear of polymer processing equipment and may not suffer from size reduction during processing, both of which occur when inorganic fibers or fillers are used. Although the absolute property increase when using organic fibers is not anticipated to be nearly as high as when using inorganic fibers, the specific proper-

ties are anticipated to be high owing to the much lower density of the organic fibers.

In short-fiber reinforced polymer composites, the integrity of the fiber/matrix interface needs to be high for efficient load transfer. Ideally, the molten polymer would spread over and adhere to the fiber, thus creating a strong adhesive bond. Inorganic fibers like glass and cellulosic fibers have hydrophilic surfaces that make them incompatible with hydrophobic polymers. Therefore, inorganic and cellulosic fibers usually require chemical modification to increase fiber/polymer interactions [1]. The chemical modification, known as a coupling agent, acts as a “bridge” between the inorganic fiber and the organic polymer matrix. The “bridge” must adhere or bond to the fiber and, in turn, strongly interact with the polymer. When using glass fibers, the coupling agent has a hydrophilic side that is compatible with the fiber and a hydrophobic side that is compatible with the polymer. In glass fibers, the coupling agent reacts with the surface of the glass forming covalent bonds. Without the coupling agent, there is simply adhesion of the polymer to the glass through weak bonding,

<sup>☆</sup> Mention of trade names or commercial products in this article is solely for the purpose of providing specific information and does not imply recommendation or endorsement by the US Department of Agriculture.

<sup>\*</sup> Corresponding author. Fax: +1 301 504 5992.

*E-mail address:* [baronej@ba.ars.usda.gov](mailto:baronej@ba.ars.usda.gov) (J.R. Barone).

i.e., van der Waals or induction interactions. Organic fibers may offer the possibility of covalently bonding the matrix polymer to the fiber either directly or through a similar type of chemical “bridge” and the chemistry may be easier. Covalent bonds are much stronger than induction or van der Waals interactions so a covalently bonded interface would be advantageous [2].

Most studies of naturally occurring organic fibers concentrate on cellulose-based fibers obtained from renewable plant resources such as wood [3–11], cotton [12], flax [13], sisal [14,15], jute [16], hemp [17], ramie [18], and bamboo [19]. Lundquist et al. [3] were able to get modulus increases of about 4 times and yield stress increases of about 2 times using cellulose fibers of ca. 17  $\mu\text{m}$  diameter and aspect ( $L/D$ ) ratio of ca. 76. However, the increase required a deviation from tradition melt processing techniques. The polymer matrices used to make the composites can be synthetic or naturally-derived and thermoplastic or thermosetting. There is much work reported on making natural fiber reinforced composites from epoxidized soybean oil or soy based polyurethane [12,20]. Not only are those matrices naturally-derived but processing can occur at low temperature so as to avoid fiber degradation. Synthetic thermosetting epoxies with flax fibers [21] and polyurethanes with sisal fibers [22] that can be molded at low temperature have also been used. These techniques carefully avoid processing at temperatures similar to the degradation temperature of the fibers.

Conventional synthetic thermoplastic polymers, like polyethylene (PE) and polypropylene (PP) have also been used to make natural fiber composites. Colom et al. [4] prepare HDPE/wood fiber composites using a compounding step at 160 °C in a roll mill and a molding step at 150 °C in a compression molder for up to 20 min. This is a more traditional polymer composite processing method. Colom et al. are only able to get property increases from cellulose fibers after treatment with a silane coupling agent to increase fiber/polymer interactions. These researchers observe modulus increases of about 2 times and yield stress increases of about 1.6 times in HDPE composites over a fiber loading range of 10–40 weight percent. However, the aspect ratio of the fibers is short at  $L/D \sim 9$ . Eboatu et al. [23] compound oil palm particles in PP on an extruder at 190 °C. Kuan et al. [24] incorporate wood fiber into HDPE on a laboratory extruder while Sameni et al. [25] mix wood fiber into PP on a Brabender mixing head. Ali et al. [26] prepare sisal fiber composites on a Haake mixing head and show a property increase with increasing fiber aspect ratio at constant 20 wt% loadings. The sisal fibers have diameters of 40–150  $\mu\text{m}$  and aspect ratios of 50–135.

There are some studies detailing the incorporation of organic fibers in plasticized polymers. Oksman et al. [27] mix flax fibers into plasticized polylactic acid (PLA) to obtain composites with increased mechanical properties

over the plasticized PLA alone. At room temperature, PLA is in a glassy state and plasticizing lowers the glass transition temperature to below room temperature, giving plasticized PLA thermal and mechanical properties similar to PP. The composites are compounded on an extruder at temperatures of about 180 °C, which is a typical temperature for polyolefin processing. Jana and Prieto [5] plasticize polyphenylene ether (PPE) to reduce the glass transition temperature. PPE is processed at around 260 °C, which is well above its glass transition of 212 °C. Plasticizing allows for processing at 200–220 °C with wood fibers so as to minimize fiber degradation. In the case of Oksman et al. and Jana and Prieto, the composite of plasticized polymer and cellulose fiber has increased properties over the plasticized polymer alone. However, the modulus and tensile strength of the plasticized polymer/cellulose fiber composite are comparable to that of the virgin, unplasticized polymer. The advantage of plasticization then is to lower the processing temperature and to increase “toughness” as manifested in a larger elongation to break and increased impact properties.

There are a few studies detailing composites made from protein fibers obtained from agricultural resources. Madera-Santana et al. [28] have prepared leather short-fiber reinforced PVC composites. Madera-Santana et al. show yield stress increases of up to 5 times and modulus increases of up to 150 times when using leather fibers in PVC but only after chemical treatment of the fibers. Much smaller property increases are observed at high fiber loadings without chemical modification. The leather fibers have small diameter, i.e., several microns, and aspect ratios of ca. 50.

There does not appear to be a shortage of possible sources of naturally occurring fibers that could be harvested for use in composite materials. One accessible fiber resource is the over four billion pounds of chicken feather waste generated by the US poultry industry each year [29]. The feathers are made of keratin, which contains ordered  $\alpha$ -helix or  $\beta$ -sheet structures and some disordered structures. The feather fiber fraction has slightly more  $\alpha$ -helix over  $\beta$ -sheet structure. The clear outer quill has much more  $\beta$ -sheet than  $\alpha$ -helix structure [30]. This leads to a crystalline melting point of ca. 230 °C for the outer quill compared to ca. 240 °C for the feather fiber [31]. Feather keratin has a molecular weight of about 10,500 g/mol [32] and a cysteine/cystine content of 7% in the amino acid sequence [33]. Cysteine is a sulfur containing amino acid responsible for the sulfur–sulfur bonding in the keratin.

The mechanical properties of whole feathers and feather rachis (i.e., the quill or shaft of the feather) have been measured for several species of birds. Purslow and Vincent [34] measure the elastic modulus of primary feather shafts from pigeons, with and without the medulla (inner quill) using a bending test. The modulus val-

ues obtained are 7.75–10 GPa on dehydrated feather shafts. The values are lower after removal of the medulla. Fraser and MacRae report modulus and peak stress values of Laysan albatross feather at 65% relative humidity as 5.2 GPa and 200 MPa, respectively [35]. The values are lower at 100% humidity, with modulus being 3.4 GPa and peak stress 100 MPa. Bonser and Purslow [36] use tensile testing to obtain the Young's modulus of the feather quill or shaft from a variety of birds. All of the values are about 2.5 GPa at room temperature and humidity. Cameron et al. show that the modulus of feather rachis is higher in birds capable of flight than it is in terrestrial birds [37]. From tensile tests, the modulus of swan and goose feather rachis is 2–4 times higher than for ostrich feather rachis. In addition, these researchers show that the modulus increases along the length of the feather shaft, with the lowest value near the skin and the highest value at the tip. X-ray diffraction measurements show more keratin molecule orientation further out along the rachis, which is the origin of the higher measured moduli. Swan and goose feather rachis have modulus values of 2.5–5 GPa while ostrich has a modulus value of about 1.5 GPa at 50% relative humidity.

Much less is known about the physical properties of the fiber portion of the feather. While there is much data on the quill portion, the quill is predominantly  $\beta$ -sheet protein structure and may differ in properties from the fiber [30]. Recently, George et al. [38] reported the mechanical properties for turkey feather fiber. Turkey feather fiber varies in dimension and properties depending on the position on the feather shaft. Fiber located closer to the bird is smaller in diameter and has lower physical properties than fiber from further out on the rachis. So the fiber shows the same trend in physical properties as the rachis. George et al. show that the fibers closer to the bird have an average denier of 55.2 g/9000 m, average tenacity at break of 0.36 g/denier, average strain at break of 16.43%, and average modulus of 4.47 g/denier. The fibers further out on the shaft have values of 142 g/9000 m, 0.83 g/denier, 7.96%, and 15.55 g/denier, respectively. If the density of the turkey feather fiber is known, the denier values could be converted to fiber diameters and then the physical property data converted to stress units. In addition, George et al. note that the fibers closer to the bird are not straight but branched and this may affect the reported denier values by making them artificially high. Turkey feather fiber is much larger in diameter than poultry feather fiber. Also, mechanical properties are measured on fiber bundles, not individual fibers, which may affect results.

Composite materials have been prepared from poultry feather fiber. Hamoush and El-Hawary prepared feather-fiber reinforced concrete at 1–3 vol% of fiber and found that the workability of the mix is low compared to ordinary cement and more plasticizer is needed [39]. The

physical properties of the feather fiber concrete are lower than ordinary concrete because of the large amount of plasticizer used. The origin of the low workability may lie in a viscosity modification due to fiber addition as well as the absorption of water by the protein fiber. Concrete is typically 15–20 vol% water [40] so the fiber may be absorbing water and the authors perhaps should have pursued the addition of water rather than plasticizer to increase workability. Water is lost when the concrete dries and physical properties may have been maintained. Bullions et al. [41,42] prepare composites of kenaf bast, wood pulp, and poultry feather fiber with polypropylene using a wetlay process. For feather fiber/PP composites, modifying PP with maleic anhydride to increase fiber/polymer interactions increases the physical properties of the composites. Dweib et al. [20] use a vacuum-assisted resin transfer molding process to mold recycled paper/feather fiber composites from epoxidized soybean oil. The composites are processed at room temperature to avoid fiber degradation. Schuster compounds feather fiber in polypropylene on an extruder at 200 °C [43] and observes increased hardness and heat distortion temperature. Concurrently, tensile stress and modulus are maintained but impact strength and ultimate elongation decrease with the addition of fiber. Schuster uses 2% bismaleinhydride as a coupling agent. Schuster also separates out the straight fibers from the branched fibers and notices no difference in composite solid-state properties but claims the branched fibers are more difficult to process in the melt state.

In this paper, keratin feather fiber ranging in length from 0.0053 to 0.2 cm is incorporated into low-density polyethylene at percentages of 0–50% wt. The composites are mixed in a Brabender mixing head. Following mixing, tensile bars are prepared and tested in uniaxial tension to assess elastic modulus, yield stress, and yield strain. Scanning electron micrographs of the fracture surfaces denote fiber/polymer interactions and fiber orientation.

## 2. Experimental

### 2.1. Keratin feather fiber

Keratin feather fiber is obtained from Featherfiber<sup>®</sup> Corporation (Nixa, MO). The keratin feather fiber is cleaned and separated from the quill fraction according to a process developed and patented by the USDA [44]. Currently, Featherfiber<sup>®</sup> Corporation is the only known commercial supplier of feather fiber material. While there is much raw feather material available from poultry processors, the feathers would have to be cleaned and separated to obtain the fiber. The possibility of different fibers possessing different properties has been alluded to previously. So it may be possible to tailor

composite properties by separating out fibers from different parts of the feather or from different feathers. In practice, the fibers used are a combination of all of the fiber obtained from the poultry feathers, which is a more practical way to produce composites from poultry feather fiber.

The feather fiber is semi-crystalline and has a constant diameter of approximately 5  $\mu\text{m}$ . The density of feather fiber is determined by displacing a known volume and weight of ethanol with an equivalent amount of fiber. A density value of 0.89  $\text{g}/\text{cm}^3$  is obtained. The fiber lengths received range in length from ca. 0.32 to 1.3 cm so uniform lengths are obtained through grinding and sieving the as-received fraction.

Fibers of 0.02, 0.1, and 0.2 cm lengths are made by grinding feather fiber using a Retsch ZM 1000 centrifugal grinder. The rotational velocity of the instrument is 15,000 rpm and contains a torque feedback so as to not feed in too much material and overload the motor. The fiber is fed in slowly to avoid motor overload and to minimize frictional heating of the instrument and the fiber. Smaller fiber lengths are made by grinding the fiber on a Retsch PM 400 ball mill. Feather fiber is loaded into 500 ml stainless steel grinding vessels so that it occupies about a quarter of the volume. The grinding media are four 4 cm stainless steel spheres for a total of 1132 g grinding media. Grinding proceeds at 200 rpm for 30 min.

Each ground fraction is sieved on a Retsch AS 2000 vibratory mill. For the longer fiber lengths, 1 cm diameter glass beads are used as sieving aids to aid the separation process. Sieving occurs at a constant frequency but amplitude and time can be varied. The material is loaded into the top sieve of the stack. The sieving stack contains eight sieves with hole sizes from 0.0710 to 0.0038 cm. Sieving at an amplitude of 1.0 (arbitrary instrument scale) for 60 min effectively separates the “fines” from the desired average fiber length.

## 2.2. Composite preparation

The matrix material is a low-density polyethylene (LDPE) commercially available from Dow called LD133A. The LDPE has a melt flow index (MFI) of 0.22 g/10 min at 190 °C and 2.16 kg and a density of 0.92  $\text{g}/\text{cm}^3$  in the solid-state. The melting temperature and percent crystallinity of LD133A is determined from differential scanning calorimetry according to ASTM D3417 and ASTM D3418 using a TA Instruments DSC 910S. The melting temperature is 112 °C and the percent crystallinity is 45%.

The total sample weight of each composite is 35 g. Composites are prepared by first adding the LDPE into a Brabender mixing head set at 150 °C and rotating at 50 rpm. Immediately after adding the LDPE, the respective amount of feather fiber is added into the mixing

head. Feather fiber loadings range from 0 to 50 wt%. Higher loadings take approximately 2 min to load into the mixing head. The melt temperature is monitored independently and ranges from 171 °C for the pure polymer to 183 °C for the highest fiber loading. The total mixing time for each composite is 15 min.

Following mixing, each sample is sandwiched between Teflon-coated aluminum foil and pressed into three thin sheets in a Carver Press Autofour/30 Model 4394 at 160 °C, 133446 N for 18 s. The film is then removed and cooled under an aluminum block until it reaches room temperature. After pressing, each thin film is inspected to note feather fiber dispersion. Good dispersion is observed in all cases except the 50 wt% loading, which appears to be overloaded as evidenced by some agglomeration of fibers.

To examine the effect of mixing, LDPE samples are prepared without mixing. No difference in physical properties is observed between mixed and unmixed LDPE after testing.

To prepare samples for testing, the three thin sheets are cut into quarters, stacked on top of each other, sandwiched between Teflon-coated aluminum foil, and pressed in the Carver Press at 160 °C and 8896 N for 2 min. After pressing, the films are cooled under an aluminum block until they reach room temperature. This results in films approximately 0.3 cm in thickness. Type IV dogbone samples for testing according to ASTM D638 are machined from the films.

## 2.3. Composite testing

Composite samples are allowed to sit at ambient conditions for one week before testing. Uniaxial tensile testing is performed using a Com-Ten Industries 95 RC Test System. Test speeds,  $v$ , from 2.5 to 22.9 cm/min (1 to 9 in./min) are used. Physical properties have a weak dependence on test speed, i.e.,  $(\log E) \sim (\log v)^{0.09}$  and  $(\log \sigma_y) \sim (\log v)^{0.03}$ . The data for the applied testing speed of 12.7 cm/min (5 in./min) is reported. A minimum of three samples of each composite is tested. Elastic modulus,  $E$ , is defined as the initial linear portion of the stress-strain curve, after correcting for the “toe” region. This portion of the curve is fit to a first order polynomial and  $E$  is obtained from the slope. The yield stress,  $\sigma_y$ , and yield strain,  $\epsilon_y$ , are defined as the stress and strain at the “peak” of the stress-strain curve. The composites break at this point and the polymer control samples yield significantly.

## 2.4. Microscopy

The fracture surfaces are excised from the failed tensile bars using a scalpel blade and transferred into a modified specimen carrier. The specimen carrier is known as an “indium vise” because the dissected pieces

are clamped between sheets of indium metal and plunge cooled in liquid nitrogen to  $-196\text{ }^{\circ}\text{C}$ . The cooled holder is then transferred to an Oxford CT1500 HF cryo-preparation system attached to a Hitachi S-4100 scanning electron microscope (SEM). The sample temperature is raised to  $-90\text{ }^{\circ}\text{C}$  for 10 min to remove surface water from the sample surface. The sample is then cooled to below  $-120\text{ }^{\circ}\text{C}$  and coated with approximately 5 nm of platinum metal using a magnetron sputter coater. Coated samples are transferred to the cold stage in the SEM at  $-170\text{ }^{\circ}\text{C}$  and observed with an electron beam accelerating voltage of 2 KV.

### 3. Results

Fig. 1 shows the elastic modulus,  $E_c$ , and the specific modulus,  $E_c/\rho_c$ , of the composites made from 0.1 cm long fibers. The composite density,  $\rho_c$ , is determined from the equation

$$\rho_c = \left( \frac{w_f}{\rho_f} + \frac{w_p}{\rho_p} \right)^{-1}, \quad (1)$$

where  $w$  is weight fraction,  $f$  denotes fiber and  $p$  denotes polymer [1]. Eq. (1) assumes there is no void volume in the composite from processing. Independent measurement of the composite density shows a slightly higher density than that predicted by Eq. (1). This could be the result of compression molding the composites to obtain tensile bars or of experimental error in the measurements. The modulus is normalized by the composite density with units of  $\text{kg}/\text{m}^3$ . The weight fraction of fiber

is converted to volume fraction using the equation  $\phi_f = (\rho_c - \rho_p)/(\rho_f - \rho_p)$ .

Fig. 2 shows the yield stress,  $\sigma_y$ , and yield strain,  $\epsilon_y$ , behavior for the composites made from 0.1 cm fiber lengths (fiber aspect ratio,  $L/D = 200$ ) over the entire feather fiber loading range. Yield stress noticeably increases as feather fiber loading increases. The yield strain decreases as fiber loading increases.

Fig. 3 shows the effect of fiber aspect ratio on elastic modulus and yield stress. All of the data are from

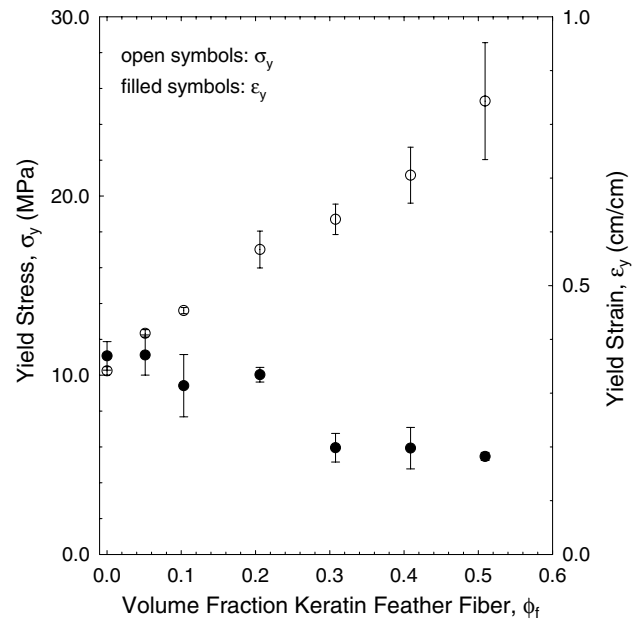


Fig. 2. Composite yield stress and strain versus volume fraction of 0.1 cm keratin feather fiber.

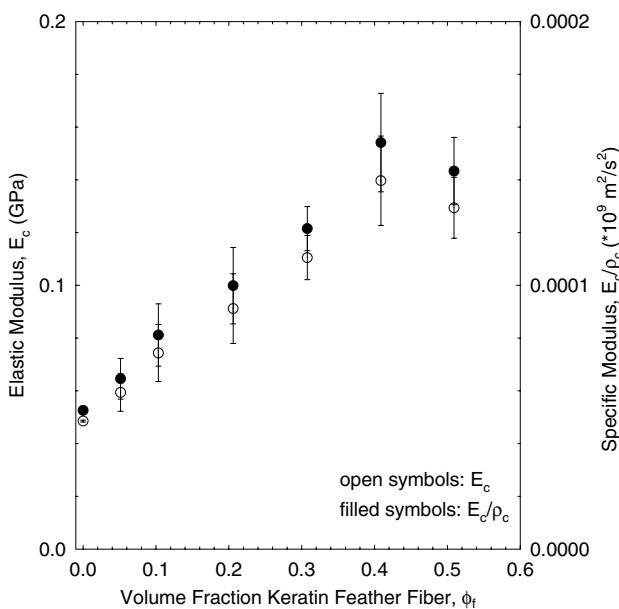


Fig. 1. Composite elastic modulus and specific modulus versus volume fraction of 0.1 cm keratin feather fiber.

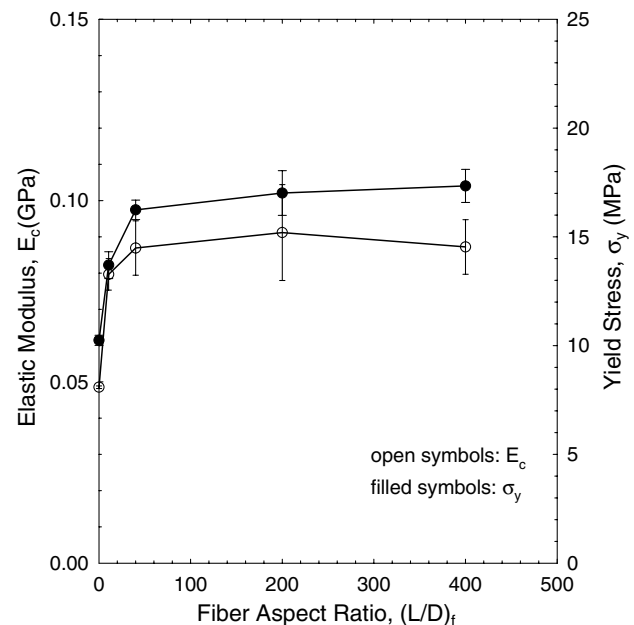


Fig. 3. Composite elastic modulus and yield stress versus fiber aspect ratio at constant 20 wt% fiber loading.

composites loaded to 20 wt% (20.6 vol%) feather fiber. There is an indication that modulus and yield stress increase as fiber aspect ratio increases and that beyond a critical fiber aspect ratio of approximately 50 the physical properties are unchanged.

#### 4. Discussion

The results show that reinforcement of a polymer matrix can be achieved with keratin feather fiber. In Fig. 1, there is an observed increase in elastic modulus of almost 3 times over the keratin feather fiber loading range. Fig. 2 shows that the yield stress increases by a factor of 2.5 over a fiber volume fraction range of 0–0.51. A micromechanical approach to predict the strength of composites is

$$\sigma_c = k\phi_f\sigma_f + \phi_p\sigma_p, \quad (2)$$

where  $k$  is a term sometimes referred to as the “stress efficiency factor” [26]. The term  $k$  is a function of the fiber/matrix adhesion, which governs the transfer of stress from the polymer matrix to the fiber, fiber orientation relative to loading direction, fiber shape, and fiber aspect ratio. It is assumed that all of the fibers are of the same circular cross-section and constant aspect ratio of  $L/D = 200$ , which, from Fig. 3, indicates that  $L > L_c$  or the fiber is sufficiently long to maximize fiber loading. Table 1 shows the  $k$  values as a function of fiber volume fraction as determined from Eq. (2). The value of  $\sigma_p$ , determined experimentally, is 10.24 MPa. The  $\sigma_f = 200$  MPa data of Fraser and MacRae is also used. One factor that could affect the micromechanical analysis is the lack of physical property data for the keratin feather fibers used. However, any deviation from the literature values would be reflected in the adjustable parameters in the micromechanical analysis. The  $k$  values obtained are not zero or negative but are not 1, which would indicate perfect adhesion and all fibers oriented in the deformation direction [1]. The low  $k$  values indicate that all of the fibers are not oriented in the loading direction and/or fiber/polymer interactions are not maximized.

To further investigate the orientation of the fibers and the fiber/polymer interactions, the fracture surfaces

Table 1  
Stress efficiency factor,  $k$ , for LD133A composites with  $L/D = 200$  feather fiber

$\phi_f$ (%)	$k$
0	0
10.3	0.153
20.6	0.133
30.8	0.161
40.9	0.135
50.9	0.159

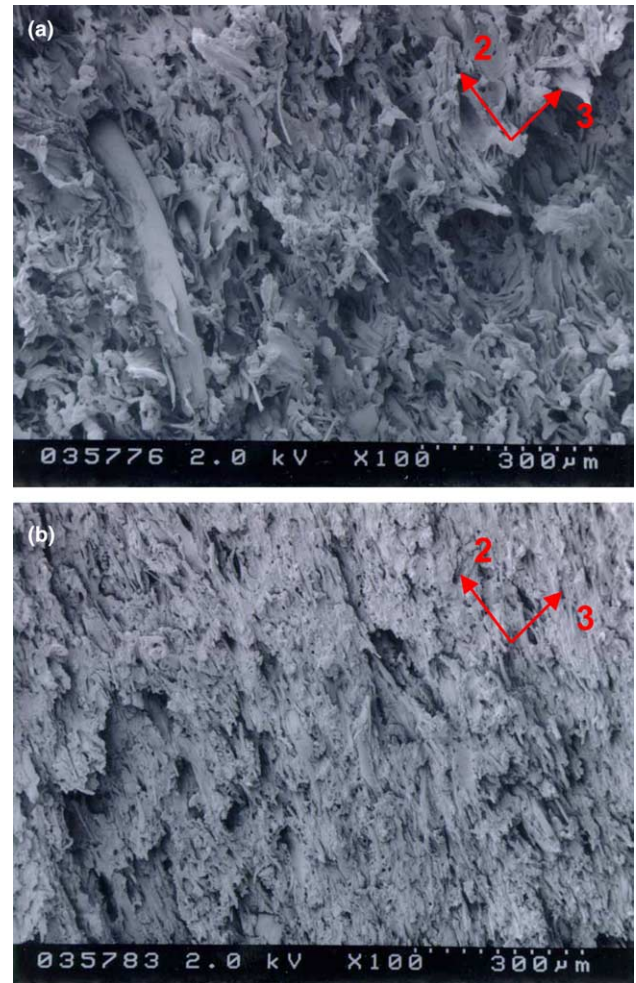


Fig. 4. (a) 10 wt% and (b) 40 wt% 0.1 cm keratin feather fiber in LD133A LDPE. Scale bar is 300  $\mu$ m.

of the tensile bars are imaged using SEM. Figs. 4(a) and (b) are micrographs of the fracture surfaces at 10 and 40 wt% (10.3 and 40.9 vol%), respectively. The loading direction 1 (tensile bar gage length direction) is into the paper. The transverse directions 2 (width of tensile bar) and 3 (thickness of tensile bar) are marked on the micrographs. There is a fair amount of fibers oriented in the transverse direction 2. Voids and fibers in direction 1 also are evident. Observation of Fig. 4(b) shows that the voids are about the diameter of the fibers so the voids may represent volumes once occupied by fibers. It would seem that if the voids are the result of processing anomalies, then the voids would have a wider size distribution. The fiber length is 0.1 cm which is 1/3 the thickness value so not much orientation in the 3 direction would be expected. Fiber length reduction is difficult to assess because the fibers are only partially exposed. The fibers are well dispersed, which is important to obtain good physical properties.

Figs. 5(a) and (b) show the same fracture surfaces as in Fig. 4 but at a higher magnification. There is some fiber/

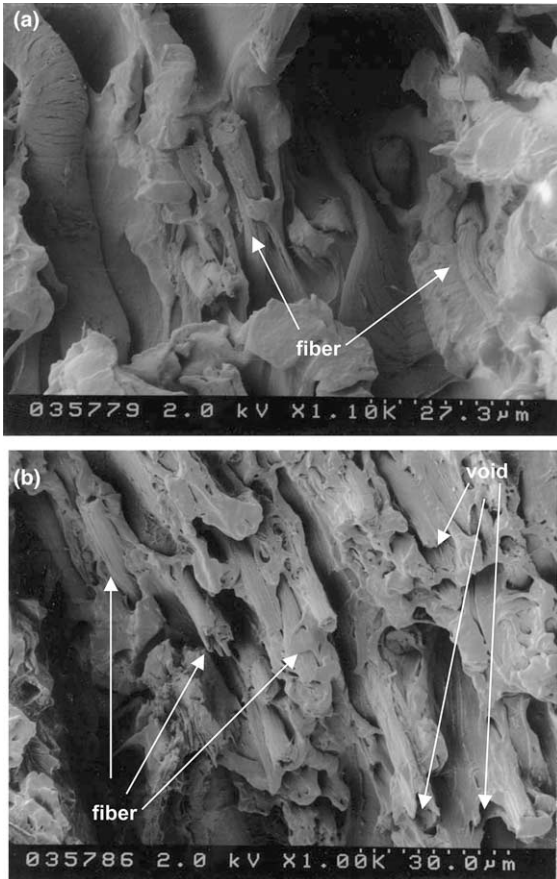


Fig. 5. (a) 10 wt% and (b) 40 wt% 0.1 cm keratin feather fiber in LD133A LDPE. Scale bar is 30  $\mu\text{m}$ .

polymer interaction as shown by the matrix adhering to the fibers to some degree. Some matrix deformation occurs along with the fibers as the fibers are pulled. There is some fiber pullout as noticed by the voids left and the exposed fibers. Some of the fibers are fractured in the same fracture plane as the polymer, which would indicate strong fiber/polymer interactions. This is shown more clearly in Fig. 6, which is a high magnification of the 40

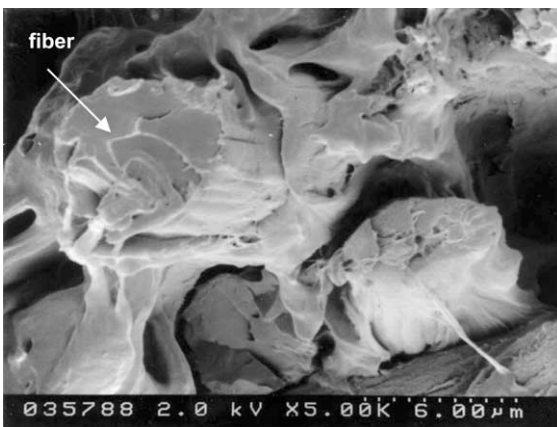


Fig. 6. 40 wt% 0.1 cm keratin feather fiber in LD133A LDPE. Scale bar is 6  $\mu\text{m}$ .

wt% composite fracture surface. Here, the fiber is wetted by the polymer and the fiber fragment length is not very long, indicative of good adhesion [26,27].

Also shown in Fig. 2 is the onset strain for yielding,  $\epsilon_y$ . The yield strain trend is indicative of a transition of the material behavior from ductile to brittle. Referring to Fig. 4, at 10 wt%, the fracture topography is ductile, with localized drawing of the polymer. At higher fiber loadings, the fracture topography becomes flatter with less localized polymer drawing.

The amino acid sequence of feather keratin shows that the protein has 40% hydrophilic and 60% hydrophobic groups [33]. The keratin feather fiber should be compatible with hydrophobic polymers to some degree. The intrinsic surface roughness of the fibers increases the surface area by a factor of about 2.2 over a perfectly smooth fiber. The extra surface area factor was estimated from length scale observations from SEM micrographs of individual fibers. The possibility of strong chemical compatibility and lots of available fiber surface area may increase the fiber/surface interactions over smooth inorganic fibers or cellulose-based fibers.

Keratin contains “bound water” [45] that is strongly hydrogen-bonded in the protein structure and seems to persist to high temperatures as evidenced by DSC studies on the fibers [31]. The weaker fiber/polymer interactions, evidenced by the voids representative of fiber pull-out, may be a result of fibers that contain more bound water during processing. The water-containing fibers would not be very compatible with the hydrophobic LDPE matrix. The stronger fiber/polymer interactions may be a result of fiber drying during processing and strong interaction of the LDPE matrix with the hydrophobic portions of the keratin. Therefore, low  $k$  values are the result of less than optimum fiber orientation and fiber/polymer interactions because (1) some of the fibers are not oriented in the deformation or 1-direction, (2) some of the protein fiber is hydrophilic and therefore incompatible with the hydrophobic polymer, (3) some bound water may make portions of the fiber incompatible with the polymer.

Fig. 3 shows a plot of the effect of fiber aspect ratio,  $(L/D)_f$ , on composite mechanical properties. Fiber aspect ratio is important for maximum load transfer from the polymer matrix to the fiber. If there is strong fiber/polymer adhesion, the application of a tensile load in the fiber direction will cause a shear stress to develop in the polymer near the interface. The shear stress will cause the polymer to plastically flow around the fiber. The maximum interfacial shear stress,  $\tau_{\text{max}}$ , would be related to the shear yield stress of the matrix, i.e.,  $\tau_{\text{max}} \sim \tau_{y,p}$ . It may not be exactly the same value if the physical properties of the polymer in a confined space differ from the bulk physical properties. If there is weak adhesion, then the fiber will slide along the interface and “pull-out”. In other

words, if there is weak adhesion, shear deformation will debond the polymer from the fiber and the shear stress originates from polymer/fiber sliding friction. In either case, the shear stress at the interface,  $\tau$ , is important to describe the load transfer. A force balance across the fiber/polymer interface yields [1]

$$\left(\frac{L_c}{D}\right)_f = \frac{\sigma_{y,f}}{2\tau}, \quad (3)$$

where  $\sigma_{y,f}$  is the yield stress of the fiber. From Fig. 3, composite yield stress is maximized at fiber aspect ratios greater than 50, which corresponds to a critical fiber length,  $L_c$ , of 0.025 cm. Assume that the critical fiber length is the length necessary to load the fiber to its yield stress. Using  $(L_c/D)_f = 50$  and  $\sigma_{y,f} = 200$  MPa yields  $\tau = 2$  MPa. The yield stress of the polymer is  $\sigma_{y,p} = 10$  MPa. Assuming that the composite is incompressible and the fiber and matrix are strained equally,  $\tau_{\max} \sim \sigma_{y,p}/3 \sim 3.3$  MPa. Therefore, the fiber may be sufficiently long to load the fiber to its yield stress by load transfer through the polymer matrix plastically flowing around it. The micrographs support this conclusion, i.e., some of the fibers have been drawn out with the polymer and some have broken in the fracture plane. The 2 MPa value (<3.3 MPa) may be a manifestation of the fibers that have pulled out. So some of the interfacial stress originates in the matrix deformation and some in polymer/matrix friction during sliding indicating that fiber/polymer interactions are good but not maximized.

## 5. Conclusions

In this paper, it is shown that keratin feather fiber acts to reinforce the LDPE polymer matrix. The feather fiber fraction of the feather waste is used and yields fibers of small constant diameter. Large fiber aspect ratios can be obtained easily with grinding. Physical property testing and microscopy show some interaction between the fiber and polymer without the need for coupling agents or chemical treatment of the fibers. Not only is it imperative to use a fiber of higher modulus, but it is important to have good fiber/polymer interaction to obtain reinforcement from fibers. The keratin feather fibers can be directly incorporated into the polymer using standard thermomechanical mixing techniques. The density of the composite upon introduction of keratin feather fiber is not increased, but reduced by 2%.

## Acknowledgements

The authors thank Eric Erbe of the USDA-ARS for the SEM experiments on the composites. The comments of the reviewers are also greatly appreciated.

## References

- [1] Chawla KK. Composite materials. Springer; 1987. p. 200–202; 79–86.
- [2] Vincent J. Structural biomaterials. Princeton University Press; 1990. p. 43.
- [3] Lundquist L, Marque B, Hagstrand P-O, Leterrier Y, Manson J-AE. Novel pulp fibre reinforced thermoplastic composites. *Comp Sci Tech* 2003;63:137–52.
- [4] Colom X, Carrasco F, Pages P, Canavate J. Effects of different treatments on the interface of HDPE/lignocellulosic fiber composites. *Comp Sci Tech* 2003;63:161–9.
- [5] Jana SC, Prieto A. On the development of natural fiber composites of high-temperature thermoplastic polymers. *J Appl Pol Sci* 2002;86:2159–67.
- [6] Jana SC, Prieto A. Natural fiber composites of high-temperature thermoplastic polymers: effects of coupling agents. *J Appl Pol Sci* 2002;86:2168–73.
- [7] Nunez AJ, Kenny JM, Reboredo MM, Aranguren MI, Marcovich NE. Thermal and dynamic mechanical characterization of polypropylene-woodflour composites. *Pol Eng Sci* 2002;42: 733–42.
- [8] Oksman K, Clemons C. Mechanical properties and morphology of impact modified polypropylene-wood flour composites. *J Appl Pol Sci* 1998;67:1503–13.
- [9] Schneider JP, Myers GE, Clemons CM, English BW. Biofibers as reinforcing fillers in thermoplastic composites. *J Vinyl Add Tech* 1995;1:103–8.
- [10] Maldas D, Kokta BV. Composite molded products based on recycled polypropylene and woodflour. *J Therm Comp Mat* 1995;8:420–34.
- [11] Selke SE, Wichman I. Wood fiber/polyolefin composites. *Comp Pt A* 2004;35:321–6.
- [12] Petrovic ZS, Guo A, Javni I, Zhang W. Plastics and composites from soybean oil. In: Wallenberger F, Weston N, editors. Natural fibers plastics and composites-recent advances. Kluwer Academic Publishers; 2003. p. 167–92.
- [13] Singleton CAN, Baillie CA, Beaumont PWR, Peijs T. On the mechanical properties, deformation and fracture of a natural fibre/recycled polymer composite. *Comp Pt B* 2003;34:519–26.
- [14] Jayaraman K. Manufacturing sisal-polypropylene composites with minimum fibre degradation. *Comp Sci Tech* 2003;63:367–74.
- [15] Frollini E, Paiva JMF, Trindade WG, Tanaka Razera IA, Tita SP. Plastics and composites from lignophenols. In: Wallenberger N, Weston N, editors. Natural fibers plastics, and composites-recent advances. Kluwer Academic Publishers; 2003. p. 193–225.
- [16] Rana AK, Mandal A, Bandyopadhyay S. Short jute fiber reinforced polypropylene composites: effect of compatibiliser, impact modifier, and fiber loading. *Comp Sci Tech* 2003;63:801–6.
- [17] Hughes M, Hill CAS, Hague JRB. The fracture toughness of bast fibre reinforced polyester composites. Part 1 evaluation and analysis. *J Mat Sci* 2002;37:4669–76.
- [18] Netravali AN. Ramie fiber reinforced natural plastics. In: Wallenberger F, Weston N, editors. Natural fibers plastics, and composites-recent advances. Kluwer Academic Publishers; 2003. p. 321–43.
- [19] Yamaguchi H, Fujii T. Bamboo fiber reinforced plastics. In: Wallenberger F, Weston N, editors. Natural fibers plastics, and composites-recent advances. Kluwer Academic Publishers; 2003. p. 305–19.
- [20] Dweib MA, Hu B, O'Donnell A, Shenton HW, Wool RP. All natural composite sandwich beams for structural applications. *Comp Struct* 2004;63:147–57.
- [21] Van de Weyenberg I, Ivens J, De Coster A, Kino B, Baetens E, Verpoest I. Influence of processing and chemical treatment of flax fibres on their composites. *Comp Sci Tech* 2003;63:1241–6.

- [22] Tavares MIB, Mothe CG, Araujo CR. Solid-state nuclear magnetic resonance study of polyurethane/natural fibers composites. *J Appl Pol Sci* 2002;85:1465–8.
- [23] Eboatu AN, Akpuaka MU, Ezenweke LO, Afuakwa JN. Use of some plant wastes as fillers for polypropylene. *J Appl Pol Sci* 2003;90:1447–52.
- [24] Kuan HC, Huan JM, Ma CCM, Wang FY. Processability, morphology and mechanical properties of wood flour reinforced high density polyethylene composites. *Plast Rub Comp* 2003;32:122–6.
- [25] Sameni JK, Ahmad SH, Zakaria S. Effects of processing parameters and graft-copoly(propylene/maleic anhydride) on mechanical properties of thermoplastic natural rubber composites reinforced with wood fibres. *Plast Rub Comp* 2003;31:162–6.
- [26] Ali R, Iannace S, Nicolais L. Effect of processing conditions on mechanical and viscoelastic properties of biocomposites. *J Appl Pol Sci* 2003;88:1637–42.
- [27] Oksman K, Skrifvars M, Selin J-F. Natural fibers as reinforcement in polylactic acid (PLA) composites. *Comp Sci Tech* 2003;63:1317–24.
- [28] Madera-Santana TJ, Aguilar-Vega MJ, Marquez A, Vazquez Moreno F, Richardson MOW, Cruz Machin JL. Production of leather-like composites using short leather fibers. II. Mechanical characterization. *Pol Comp* 2002;23:991–1002.
- [29] Parkinson G. Chementator: a higher use for lowly chicken feathers. *Chem Eng* 1998;105(3):21.
- [30] Schmidt WF, Jayasundera S. Microcrystalline keratin fiber. In: Wallenberger F, Weston N, editors. *Natural fibers plastics, and composites-recent advances*. Kluwer Academic Publishers; 2003. p. 51–66.
- [31] Schmidt WF, Line MJ. Physical and chemical structures of poultry feather fiber fractions in fiber process development. In: *TAPPI Proceedings: 1996 Nonwovens Conference*. p. 135–140.
- [32] Fraser RDB, MacRae TP, Rogers GE. *Keratins: their composition, structure, and biosynthesis*. Springfield: Charles C. Thomas Publisher; 1972. p. 31.
- [33] Murayama-Arai K, Takahashi R, Yokote Y, Akahane K. Amino acid sequence of feather keratin from fowl. *Eur J Biochem* 1983;132:501–7.
- [34] Purslow PP, Vincent JFV. Mechanical properties of primary feathers from the pigeon. *J Exp Biol* 1978;72:251–60.
- [35] Fraser RDB, MacRae TP. Molecular structure and mechanical properties of keratins. In: *Symposia of the Society for Experimental Biology Number XXXIV: the mechanical properties of biological materials*. Cambridge University Press; 1980. p. 211–246.
- [36] Bonser RHC, Purslow PP. The Young's modulus of feather keratin. *J Exp Biol* 1995;198:1029–33.
- [37] Cameron GJ, Wess TJ, Bonser RHC. Young's modulus varies with differential orientation of keratin in feathers. *J Struct Biol* 2003;143:118–23.
- [38] George BR, Evazynajad A, Bockarie A, McBride H, Bunik T, Scutti A. Keratin fiber nonwovens for erosion control. In: Wallenberger F, Weston N, editors. *Natural fibers plastics, and composites-recent advances*. Kluwer Academic Publishers; 2003. p. 67–81.
- [39] Hamoush SA, El-Hawary MM. Feather fiber reinforced concrete. *Conc Int: Design Const* 1994;16:33–5.
- [40] Smith WF. In: *Principles of materials science and engineering*. McGraw-Hill Inc; 1996. p. 798.
- [41] Bullions TA, Hoffman D, Price-O'Brien J, Loos, AC. Feather fiber/cellulose fiber/polypropylene composites manufactured via the wetlay papermaking process. In: *International Nonwovens Technical Conference (INTC2003)*. Baltimore, MD; September 15–18, 2003.
- [42] Bullions TA, Gillespie RA, Price-O'Brien J, Loos AC. The effect of maleic anhydride modified polypropylene on the mechanical properties of feather fiber, kraft pulp, polypropylene composites. *J Appl Pol Sci* 2004;92:3771–83.
- [43] Schuster J. Polypropylene reinforced with chicken feathers. In: *14th International Conference on Composite Materials*. San Diego, CA; July 14–18, 2003.
- [44] Gassner G, Schmidt W, Line MJ, Thomas C, Water, RM. Fiber and fiber products from feathers. United States Patent No. 5,705,030, 1998.
- [45] Feughelman M. *Mechanical properties and structure of alpha-keratin fibres*. University of New South Wales Press; 1997.